Nuclear Activity in Galaxies Across Cosmic Time
Proceedings IAU Symposium No. 356, 2019
M. Pović, P. Marziani, J. Masegosa, H. Netzer, S. H. Negu & S. B. Tessema, eds.
doi:10.1017/S1743921320002574

Predicting the emission profile and estimation of model parameters for some nearby LLAGN using accretion and jet models

Bidisha Bandyopadhyay[1], Fu-Guo Xie[2], Neil M. Nagar[1], Dominik R. G. Schleicher[1], Venkatessh Ramakrishnan[1], Patricia Arévalo[3], Elena López[3] and Yaherlyn Diaz[3]

[1]Departamento de Astronomía, Facultad Ciencias Físicas y Matemáticas, Universidad de Concepción, Av. Esteban Iturra s/n Barrio Universitario, Casilla 160-C, Concepción, Chile
email: bidisharia@gmail.com

[2]Key Laboratory for Research in Galaxies and Cosmology, Shanghai Astronomical Observatory, Chinese Academy of Sciences, 80 Nandan Road, Shanghai 200030, China

[3]Instituto de Física y Astronomía, Facultad de Ciencias, Universidad de Valparaíso, Gran Bretana No. 1111, Playa Ancha, Valparaíso, Chile

Abstract. The Event Horizon Telescope (EHT) provides a unique opportunity to probe the physics of supermassive black holes through Very Large Baseline Interferometry (VLBI), such as the existence of the event horizon, the accretion processes as well as jet formation in Low Luminosity AGN (LLAGN). We build a theoretical model which includes an Advection Dominated Accretion Flow (ADAF) and a simple radio jet outflow. The predicted spectral energy distribution (SED) of this model can be compared to observations to get the best estimates of the model parameters. The model-predicted radial emission profiles at different frequency bands can be used to predict whether the inflow can be resolved by the EHT or other telescopes. We have applied this method to some nearby LLAGN such as M84, NGC 4594, NGC 4278 and NGC 3998. We also estimate the model parameters for each of them using high resolution data from different surveys.

Keywords. accretion, accretion disks, black hole physics, Galaxy: nucleus

1. Introduction

The detection of the photon ring around the black hole in the nucleus of M87 (EHT Collaboration 2019) with the Event Horizon Telescope (EHT) using very long baseline interferometric (VLBI) techniques has opened a new window to probe regions in the extreme proximity of supermassive black holes. This advancement in science and technology has not only enabled us to test Einstein's theory of General Relativity but also to probe regions in the accretion flow which were unresolvable before. It is thus of profound importance to investigate the various physical processes involved in the accretion flow to understand the powering source of such systems. It is hence also important to probe more such systems to enhance our knowledge about the physical processes. Besides the EHT, the global 3-mm VLBI array (GMVA), which operates at 86 GHz, imaging at high resolutions (few tens of microarcsecs), will enable to observe accretion regions as well as the jet base in nearby accreting supermassive black holes.

In this proceeding we present the primary results that we obtained in our recent work (Bandyopadhyay *et al.* 2019) where we compared our modeled spectral energy distribution (SED) to the observed high resolution multi wavelength (MW) data for some selected candidates to better estimate the model parameters. Most of these systems are expected to accrete at a sub-Eddington rate and are generally radiatively inefficient with an advection dominated accretion flow and hence are also known as radiatively inefficient accretion flows (RIAFs), a subgroup of the advection dominated accretion flows (ADAFs). Due to the presence of a magnetic field and low densities, the primary emission processes contributing to the SED from the ADAF are thermal synchrotron emission, bremsstrahlung emission and comptonised emission by the thermal electrons. Often a fraction of the thermal electrons is boosted to power-law electrons which too emit via synchrotron emission. At arcsec to sub-arcsec scales, the emission from the jet base may also contribute to the observed SED and thus it is important to include the jet emission (primarily synchrotron) to match the observed data set and have a better estimate on the model parameters. We then used the estimated parameters of the accretion flow to obtain a radial profile of the emission which allows us to predict which of the sources could possibly be resolved and detected by the EHT and the GMVA.

In the following sections, there is a brief description of the equations and the parameters involved in the accretion flow. We then test our model for M87 which has been extensively studied in literature (Nemmen *et al.* 2014; Li *et al.* 2016) and also for which we now have the EHT results. We then present the results for two of the sources which we expect to be resolvable by the EHT.

2. A brief description of the model

The steady state flow equations for an ADAF with a two temperature plasma can be written in terms of the four conservation equations of mass, radial momentum, angular momentum and energy and are expressed as follows:

$$\dot{M}(R) = \dot{M}(R_{tr})\left(\frac{R}{R_{\rm tr}}\right)^s = 4\pi\rho R H|v|. \tag{2.1}$$

$$v\frac{dv}{dR} - \Omega^2 R = -\Omega_K^2 R - \frac{1}{\rho}\frac{d}{dR}(\rho c_s^2). \tag{2.2}$$

$$\frac{d\Omega}{dR} = \frac{v\Omega_K(\Omega R^2 - j)}{\alpha R^2 c_s^2}. \tag{2.3}$$

$$\rho v\left(\frac{de_i}{dR} - \frac{p_i}{\rho^2}\frac{d\rho}{dR}\right) = (1-\delta)q^+ - q^{ie}.$$

$$\rho v\left(\frac{de_e}{dR} - \frac{p_e}{\rho^2}\frac{d\rho}{dR}\right) = \delta q^+ + q^{ie} - q^-. \tag{2.4}$$

Here $R_{\rm tr}$ is the truncation radius, s is the parameter that quantifies density reductions due to outflows, $H = c_s/\Omega_K$ is the scale height, ρ is the gas density, Ω is the angular momentum of the in-falling gas, Ω_K is the angular momentum of the Keplerian orbit, v is the radial velocity of the gas, c_s is the sound speed, j is the angular momentum at the gravitational radius R_g and is an eigenvalue for the system under consideration, α is the viscosity parameter, e_e and e_i are the specific internal energies of the electrons and ions, respectively, δ is the fraction of the viscous energy (q^+) that goes into heating the electrons (Xie & Yuan 2012; Chael *et al.* 2018), q^{ie} the energy that is exchanged between electrons and ions and q^- is the energy lost via radiation. In this work, we express the mass accretion rate $\dot{M}$ in terms of the Eddingtion accretion rate $\dot{M}_{\rm Edd}$ through the dimensionless parameter $\dot{m}$ as $\dot{M}(R) = \dot{m}(R)\dot{M}_{\rm Edd}$. This parameter at R_g is equal to the Eddington ratio ($L_{\rm Bol}/L_{\rm Edd}$) in case of thin disk accretion flows but is higher for ADAF. We use the Eddington ratio as a lower limit for $\dot{m}(R_g)$. We vary this parameter

https://doi.org/10.1017/S1743921320002574 Published online by Cambridge University Press

Table 1. Model A and Model B parameter values for M87.

Model	$\dot{m}_{tr}$	δ	s	j	p_l	η	$\dot{m}_{jet}$	p_{jet}	ϵ_e	ϵ_b	ξ
Model A	4.2×10^{-4}	0.1	0.1	0.7999	3.0	0.015	1.0×10^{-8}	2.6	0.0009	0.0006	0.01
Model B	1.2×10^{-4}	0.5	0.3	1.8360	3.0	0.015	1.0×10^{-8}	2.5	0.0009	0.0006	0.01

by varying $\dot{m}(R_{\rm tr})$ (from now on $\dot{m}_{\rm tr}$) and s using eq. [2.1]. The pressure (p_i and p_e) in eq. [2.4] is the gas pressure ($p_{\rm gas} = p_i + p_e$) expressed in terms of the total pressure ($p_{\rm tot} = p_{\rm gas} + p_{\rm magnetic}$) as $p_{gas} = \beta p_{\rm tot}$.

The accretion dynamics is more complex due to turbulence, the presence of magnetic fields, hot spots and outflows. Narayan & Yi 1994; Narayan & Yi 1995; Blandford & Begelman 1999 postulated that ADAFs should have strong winds followed by the formation of jets. In this work, we use a phenomenological model (Spada *et al.* 2001) to describe the jet, which is sufficient to model the SED. It is assumed to be composed of a normal plasma, consisting of electrons and protons, with velocities determined by a bulk Lorentz factor $\Gamma_j = 10$ (typical for jets in AGN as in Lister *et al.* 2016). In this model, a fraction ξ of the electrons is boosted to a power law (power law index p_{jet}) energy distribution due to internal shocks within the jet. Parameters defining the fraction of the shock energy that goes into electrons and magnetic fields, ϵ_e and ϵ_B respectively, are included. The mass loss rate $\dot{M}_{\rm jet}$ is sensitively coupled with the jet outflow velocity $V_{\rm jet}$ (assumed to be constant for all our LLAGN) which controls the beaming effect and gas density.

Additional parameters are included when a fraction η of the thermal electrons is boosted to become power-law (p_l) electrons in the accretion flow and these electrons then emit via synchrotron emission. We then used these combined models to obtain the SED and cross match with the data.

3. Results

We initially applied our results to M87 which has a black hole mass of $6.5 \pm 0.7 \times 10^9 M_\odot$ and is at a distance of 16.8 Mpc. We used two set of model parmeter values (model A and model B) to fit to the high resolution data (Prieto *et al.* 2016) where the difference in the two models was primarily the choice of the accretion rate and the outflow parameter. We obtained a better fit to the data using the model A parameter values (see table [1] for the model parameter values) where the accretion rate agrees with the GRMHD simulation of Mościbrodzka *et al.* 2016. The SED fits with this model are shown in the left panel of fig. [1]. We then used these parameter values to obtain the radial emission profile from the ADAF at 230 GHz (EHT), 86 GHz (GMVA) and 22 GHz (EVN). The right panel of fig. [1] displays the radial profiles at the frequencies mentioned for the cases with and without the emission from non-thermal electrons in the ADAF.

We then applied our model to the high resolution data (see the Appendix in Bandyopadhyay *et al.* 2019) of the five sources (Cen A, M84, NGC 4594, NGC 3998 and NGC 4278) and obtained the best parameter value to our model to finally obtain the radial profile for these sources. Cen A which has a comparatively smaller black hole mass is also one of the nearest sources with a radio loud core. Although resolving the photon ring may not be possible, the derived radial profile of the emission suggests that a part of the accretion flow may be detectable with the EHT and also the GMVA as shown in fig. [2]. The other source whose accretion flow can be detectable by the EHT according to our analysis is NGC 3998. This source is well studied in the X-ray with various probes but is not quite radio loud. As can be seen in the right panel of fig. [2], a part of the inner accretion flow may be observable and detectable by the EHT with emission only from thermal electrons. Our analysis of all the five sources is briefly mentioned in table [3].

https://doi.org/10.1017/S1743921320002574 Published online by Cambridge University Press

Table 2. List of the sources we studied based on their mass, distance, ring sizes and Eddington ratios.

Source	$log(M_{BH}/M_{\odot})$	Distance (Mpc)	θ_{Ring} (μas)	Eddington Ratio (L_{Bol}/L_{Edd})
NGC 5128 (Cen A)	7.7	3.8	1.5	5.0×10^{-4}
NGC 4374 (M84)	8.9	17.1	4.8	5.0×10^{-6}
NGC 4594 (Sombrero, M 104)	8.5	9.1	3.6	1.5×10^{-6}
NGC 3998	8.9	13.1	6.2	1.0×10^{-4}
NGC 4278	8.6	14.9	2.7	5.0×10^{-6}

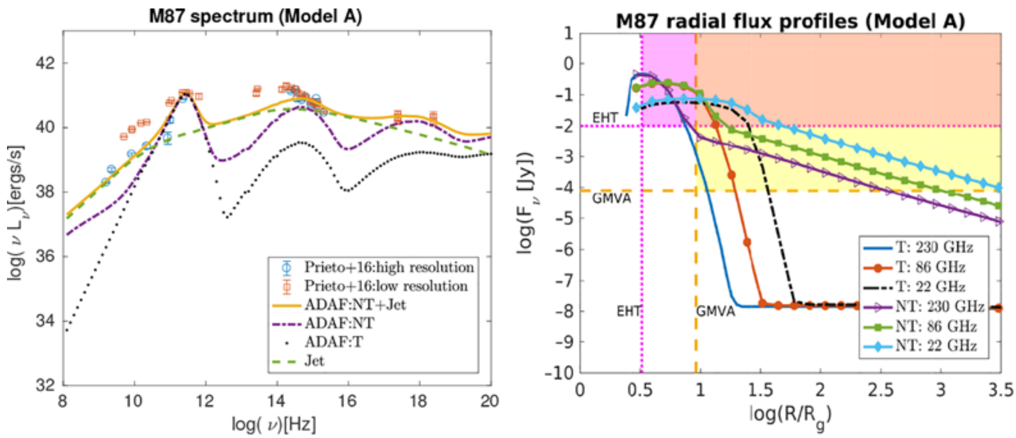

Figure 1. *Left*: SED model (Model A) fit to the high resolution data (Prieto *et al.* 2016). *Right*: The radial flux profile with the same model. The pink shaded region marks the region of detectability by the EHT only and the yellow by the GMVA while pink marks the common region of detectability.

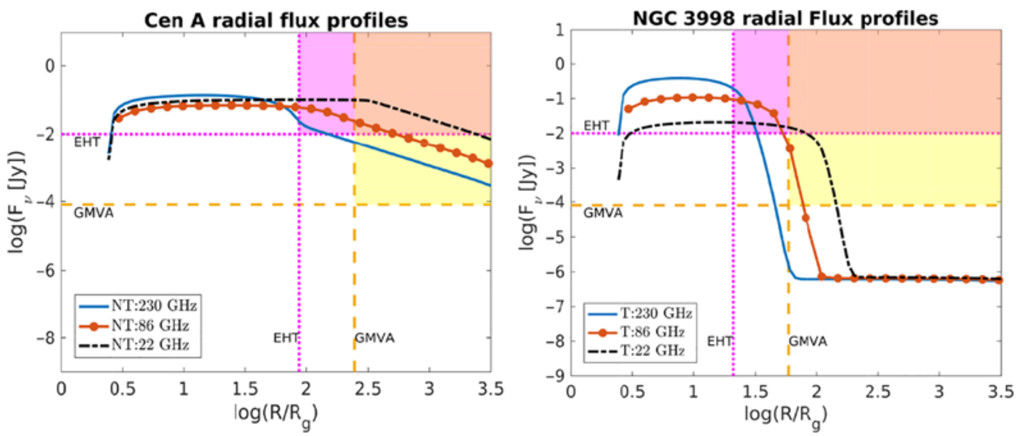

Figure 2. Radial flux profiles for Cen A and NGC 3998 respectively

4. Discussion and Conclusion

We summarize our main conclusions as follows:

• The framework described in section [2] was tested with the SED of M87 considering models A and B. The basic motivation to select these models was to consider different accretion rates and outflow parameters which compare to the values in literature (Nemmen *et al.* 2014; Li *et al.* 2016; Mościbrodzka *et al.* 2016). With these models, we

https://doi.org/10.1017/S1743921320002574 Published online by Cambridge University Press

Table 3. The table displays if the sources are detectable and resolvable by the EHT or the GMVA in an 8 hour integration time.

Source	Resolvable (EHT)	Detectable (EHT)	Resolvable (GMVA)	Detectable (GMVA)
Cen A	Yes	Partly the outer region	Outer regions	Only the outer regions
M84	Partially	No	No	No
NGC 4594	Partially	No	No	No
NGC 3998	Yes	Yes	Partially	Partly the outer region
NGC 4278	Outer regions	No	Outer regions	Outer regions

obtained the best fit to the data with a model consisting of the Jet and an ADAF with thermal plus non-thermal electrons. Model A fits the data better and the accretion rate is similar to the result of a GRMHD simulation by Mościbrodzka *et al.* 2016. Since both the models provide radial profiles which are within the observable regime of the EHT, future EHT observations may help to distinguish the two scenarios.

• We then use this model to obtain the model parameters for each of the 5 sources in our sample of galaxies by comparing the modeled SED with the observed data. Although we may not be able to resolve the region of maximum emission from the ADAF for Cen A, the flow can still be partially observed at larger radii due to the flux from non-thermal electrons. Table. [3] summarizes these predictions.

• With our model fits, we find that the radial profile of NGC 3998 is expected to be resolved very well with both EHT and GMVA. The ADAFs of M84 and NGC 4594 may be fairly resolved by EHT and not with GMVA, but may not be observable within the current flux limit of the EHT. To observe these, we need better sensitivities of the telescope and longer integration times.

References

Bandyopadhyay, B., Xie, F.-G., Nagar, N. M., Schleicher, D.R.G., Ramakrishnan, V., Arévalo, P., López, E., & Diaz, Y. 2019, *MNRAS*, 490, 4606

Blandford, R. D. & Begelman, M. C. 1999, *MNRAS*, 303, L1

Chael, A., Rowan, M., Narayan, R., Johnson, M., & Sironi, L. 2018, *MNRAS*, 478, 5209

Event Horizon Telescope Collaboration 2019, *ApJ*, 875, L1

Li, Y.-P., Yuan, F., & Xie, F.-G. 2016, *ApJ*, 830, 78

Lister, M. L., Aller, M. F., Aller, H. D., Homan, D. C., Kellermann, K. I., Kovalev, Y. Y., Pushkarev, A. B., Richards, J. L., Ros, E., & Savolainen, T. 2016, *AJ*, 152, 12

Mościbrodzka, M., Falcke, H., & Shiokawa, H. 2016, *A&A* (Letters), 586, A38

Narayan, R. & Yi, I. 1994, *ApJ*, 428, L13

Narayan, R. & Yi, I. 1995, *ApJ*, 444, 231

Nemmen, R. S., Storchi-Bergmann, T., & Eracleous, M. 2014, *MNRAS*, 438, 2804

Prieto, M. A., Fernández-Ontiveros, J. A., Markoff, S., Espada, D., & González-Martín, O. 2016, *MNRAS*, 457, 3801

Spada, M., Ghisellini, G., Lazzati, D., & Celotti A. 2001, *MNRAS* 325, 1559

Xie, F.-G. & Yuan, F. 2012, *MNRAS*, 427, 1580

Yuan, F., Peng, Q., Lu, J., & Wang, J. 1999, *ApJ*, 537, 236